



Published in final edited form as:

*Mol Pharm.* 2013 May 6; 10(5): 2008–2020. doi:10.1021/mp400046u.

## Efficient Delivery of Cell Impermeable Phosphopeptides by a Cyclic Peptide Amphiphile Containing Tryptophan and Arginine

Amir Nasrolahi Shirazi<sup>†</sup>, Rakesh Kumar Tiwari<sup>†</sup>, Donghoon Oh<sup>†</sup>, Antara Banerjee<sup>‡</sup>, Arpita Yadav<sup>‡</sup>, and Keykavous Parang<sup>\*,†</sup>

<sup>†</sup>Department of Biomedical and Pharmaceutical Sciences, College of Pharmacy, University of Rhode Island, Kingston, RI 02881, United States

<sup>‡</sup>Department of Chemistry, University Institute of Engineering and Technology, Chhatrapati Shahuji Maharaj University, Kanpur 208024, India

### Abstract

Phosphopeptides are valuable reagent probes for studying protein-protein and protein-ligand interactions. The cellular delivery of phosphopeptides is challenging because of the presence of the negatively charged phosphate group. The cellular uptake of a number of fluorescent-labeled phosphopeptides, including F'-GpYLPQTV, F'-NEpYTARQ, F'-AEEEEYGEFEAKKKK, F'-PEpYLGLD, F'-pYVNVQN-NH<sub>2</sub>, and F'-GpYEEI (F' = fluorescein) was evaluated in the presence or absence of a [WR]<sub>4</sub>, a cyclic peptide containing alternative arginine (R) and tryptophan (W) residues, in human leukemia cells (CCRF-CEM) after 2 h incubation using flow cytometry. [WR]<sub>4</sub> improved significantly the cellular uptake of all phosphopeptides. PEpYLGLD is a sequence that mimics the pTyr1246 of ErbB2 that is responsible for binding to the Chk SH2 domain. The cellular uptake of F'-PEpYLGLD was enhanced dramatically by 27-fold in the presence of [WR]<sub>4</sub> and was found to be time-dependent. Confocal microscopy of a mixture of F'-PEpYLGLD and [WR]<sub>4</sub> in live cells exhibited intracellular localization and significantly higher cellular uptake compared to that of F'-PEpYLGLD alone. Transmission Electron Microscopy (TEM) and Isothermal Calorimetric (ITC) were used to study the interaction of PEpYLGLD and [WR]<sub>4</sub>. TEM results showed that the mixture of PEpYLGLD and [WR]<sub>4</sub> formed noncircular nanosized structures with width and height of 125 and 60 nm, respectively. ITC binding studies confirmed the interaction between [WR]<sub>4</sub> and PEpYLGLD. The binding isotherm curves, derived from sequential binding models, showed an exothermic interaction driven by entropy. These studies suggest that amphiphilic peptide [WR]<sub>4</sub> can be used as a cellular delivery tool of cell-impermeable negatively charged phosphopeptides.

### Keywords

Cellular uptake; Cyclic Peptides; Nanoparticles; Phosphopeptides; SH2 domain

\*Corresponding author: K. Parang: 7 Greenhouse Road, Department of Biomedical and Pharmaceutical Sciences, College of Pharmacy, University of Rhode Island, Kingston, Rhode Island, 02881, United States; Tel.: +1-401-874-4471; Fax: +1-401-874-5787; kparang@uri.edu.

#### SUPPORTING INFORMATION AVAILABLE

Analytical HPLC data and high resolution mass spectra, and additional supporting data. This information is available free of charge via the Internet at <http://pubs.acs.org/>.

## INTRODUCTION

Peptide amphiphiles (PAs) are composed of a combination of amino acids carrying hydrophobic/hydrophilic and positively/negatively charged residues.<sup>1</sup> PAs have been found to be promising tools in drug and gene delivery due to their biocompatibility and bioactivity.<sup>2-4</sup> These compounds are not toxic to cells at their experimental concentration and are able to cross the cell-membrane because of their unique structural properties.

Hydrophobic unit of PAs can contain long chain fatty acids or amino acids with hydrophobic side chain residues. This unit generates a pocket that could be responsible for the entrapment of drugs and facilitates the internalization into the cell membrane.<sup>5</sup> At the same time, the presence of positively charged arginine facilitates the interaction between the peptide and the negatively charged phospholipids on the cell-membrane. The application of positively charged linear cell-penetrating peptides (CPPs) as drug carriers for biologically active cargos has been reported previously.<sup>6-9</sup> Polyarginines, TAT (trans-acting activator of transcription), and Penetratin have been found to enhance the cellular uptake of a diverse range of drugs.<sup>10-12</sup> Thus, the appropriate combination of amino acids in the structure of peptide determines the efficiency and function of the delivery system.

Phosphopeptides are valuable reagent probes mimicking phosphoproteins for studying protein-protein and protein-ligand interactions<sup>13,14</sup> and determination of substrate specificity of the Src homology 2 (SH2) domain,<sup>15</sup> phosphatases,<sup>16,17</sup> and phosphotyrosine binding (PTB) domains.<sup>18,19</sup> The use of phosphopeptides has been challenging due to the fact that they have limited cellular uptake because of the presence of the negatively charged phosphate group. Several chemical modifications have been used to enhance the intracellular delivery of phosphopeptides through covalent conjugation to other transporter peptides.<sup>20-22</sup> These strategies suffer from several disadvantages including multi-step synthesis of the fusion conjugates, low loading yields, and the requirement of cleavage through chemical or enzymatic reactions to release phosphopeptides.<sup>23</sup>

Peptidomimetic prodrugs have been reported for intracellular delivery of aryl phosphoramidates<sup>24</sup> and difluoromethyl phosphonates<sup>25</sup>. Arrendale and coworkers developed a (difluoromethylene)phosphoserine prodrug to deliver negatively charged phosphoserine peptidomimetic intracellularly. FOXO3a is a transcription factor that is phosphorylated by Akt1 and binds to 14-3-3-adaptor protein. The released modified phosphopeptide was able to release FOXO3a from 14-3-3 protein, leading to cell death in leukemia cells.<sup>26,27</sup> Other phosphoserine and phosphothreonine masked phosphopeptides have been evaluated in studying kinase regulation.<sup>28,29</sup>

Considering the critical roles of the phosphopeptides in cellular signaling pathways, we have previously reported amphiphilic linear peptide analogues to improve the intracellular uptake of negatively charged phosphopeptides through non-covalent conjugation.<sup>30</sup> The linear positively charged peptides were designed based on the Src SH2 domain phosphotyrosine (pTyr) binding pocket.

We introduced a new class of homochiral cyclic peptides containing arginine (R) and tryptophan (W) such as [WR]<sub>4</sub> that were appropriate carriers for a wide range of drugs.<sup>31</sup> This system showed that the optimized balance between positive charge and hydrophobicity was critical for the peptide to enhance the intracellular delivery of drugs through interaction with the cell membrane and penetration into the lipid bilayer. Cyclic [WR]<sub>4</sub> provided major advantages compared to their linear counterparts, including higher enzymatic stability, bypassing endosomal uptake, improved cell permeability, and nuclear targeting.<sup>31</sup>

In continuation of our efforts to introduce new applications of [WR]<sub>4</sub> for the delivery of biomolecules, we report here using [WR]<sub>4</sub> for improving the cellular delivery of negatively charge phosphopeptides. Addition of negatively charged phosphopeptides to the positively charged [WR]<sub>4</sub> led to the formation of nanostructures through intermolecular interactions. To the best of our knowledge, this is the first report of using a cell-penetrating cyclic peptide for cellular delivery of impermeable phosphopeptides.

## EXPERIMENTAL SECTION

### General

All amino acids were purchased from Chem-Impex International, Inc. HBTU was purchased from Oakwood products, Inc. All other chemicals and reagents were purchased from Sigma-Aldrich Chemical Co. (Milwaukee, WI). The chemical structures of final products were confirmed by high-resolution MALDI AXIMA performance TOF/TOF mass spectrometer (Shimadzu Biotech). Details of procedures and spectroscopic data of the respective compounds are presented below. Final compounds were purified on a Phenomenex Prodigy 10  $\mu$ m ODS reversed-phase column (2.1 cm  $\times$  25 cm) with a Hitachi HPLC system using a gradient system of acetonitrile (CH<sub>3</sub>CN) or methanol and water (CH<sub>3</sub>OH/H<sub>2</sub>O) (0–100%, pH 7.0, 60 min). The purity of final products (> 95%) was confirmed by analytical HPLC. The analytical HPLC was performed on a Hitachi analytical HPLC system using a C18 Shimadzu Premier 3  $\mu$ m column (150 cm  $\times$  4.6 mm) and a gradient system (water/CH<sub>3</sub>CN), and a flow rate of 1 mL/min with detection at 220 nm. Cyclic peptide [WR]<sub>4</sub> was synthesized according to our previously reported procedure.<sup>31</sup> As representative examples, the synthesis of Ac-PEpYLGLD and F'-PEpYLGLD is outlined here.

**Synthesis of Ac-PE(pY)LGLD and F'-PE(pY)LGLD**—Side chain protected peptide PE(pY)LGLD was assembled on Fmoc-Asp(OtBu)-Wang resin (740 mg, 0.54 mmol/g, 0.4 mmol) by solid-phase peptide synthesis strategy using Fmoc-protected amino acids [Fmoc-Leu-OH, Fmoc-Gly-OH, Fmoc-Leu-OH, Fmoc-Tyr(PO<sub>3</sub>tBu<sub>2</sub>)-OH, Fmoc-Glu(OtBu)-OH, and Fmoc-Pro-OH] on a PS3 automated peptide synthesizer at room temperature using 2-(1*H*-benzotriazole-1-yl)-1,1,3,3-tetramethyluronium hexafluorophosphate (HBTU) and *N*-methylmorpholine (NMM, 0.4 M) in *N,N*-dimethylformamide (DMF) as coupling and activating agents, respectively (Scheme 1). After the assembly of the side chain protected peptide sequence, the Fmoc protecting group at the *N*-terminal proline was removed using piperidine in DMF (20% v/v). The resin was washed with DCM (3  $\times$  15 mL) and MeOH (3  $\times$  15 mL) for further modification using either capping reagent (acetic anhydride) or fluorescein labeling reagent (5(6)-carboxyfluorescein isobutyrate). The resin was dried overnight under vacuum and divided into two parts. The capping reaction was carried out on the first portion using acetic anhydride ((CH<sub>3</sub>CO)<sub>2</sub>O) (953  $\mu$ L) and *N,N*-diisopropylethylamine (DIPEA) (1,742  $\mu$ L) (50/50 equiv) in DMF (10 mL). The mixture containing peptide-attached resin and reagents was shaken for 30 min, followed by washing with DMF (5  $\times$  15 mL), DCM (5  $\times$  15 mL), and MeOH (3  $\times$  15 mL), respectively. The resin was dried under vacuum at room temperature for 24 h. The second portion of the resin was swelled in DMF (2  $\times$  20 mL) for 2 h. The preactivation reaction was performed on the fluorescein reagent using a mixture of 5(6)-carboxyfluorescein isobutyrate (5 equiv), 1-hydroxy-7-azabenzotriazole (HOAt, 5 equiv)/7-azabenzotriazol-1-yloxy tripyrrolidinophosphonium hexafluorophosphate (PyAOP, 5 equiv)/DIPEA, 10 equiv) in DMF:DCM (5:1 v/v, 12 mL) for 10 min. The activated fluorescein reagent was added to the peptide-attached resin and stirred at room temperature for 3 h. After the completion of the reaction, the resin was washed by DMF (5  $\times$  15 mL), DCM (3  $\times$  15 mL), and MeOH (5  $\times$  15 mL), respectively. The protecting group (isobutyrate) was removed from the carboxyfluorescein by treating the peptide-attached resin with 20% piperidine in DMF (5  $\times$

15 mL, 25 min each). Finally, the resin was washed with DMF (5 × 15 mL), DCM (5 × 15 mL), and MeOH (5 × 15 mL), respectively, followed by drying under a high vacuum at room temperature for 24 h. The cleavage reagent R cocktail containing trifluoroacetic acid (TFA)/thioanisole/ethanedithiol (EDT)/anisole (90:5:3:2 v/v/v/v, 12 mL) was added to both portions of the resin, and the mixtures were stirred at room temperature for 2 h. The resins were filtered and washed with Reagent R (2 mL) again. The filtrates were evaporated to reduce the volume under dry nitrogen. The crude peptides were precipitated by adding cold diethyl ether (200 mL, Et<sub>2</sub>O) and centrifuged at 4000 rpm for 5 min, followed by decantation to obtain the solid precipitates. The solid materials were further washed with cold ether (2 × 100 mL) for 2 times. The peptides were lyophilized and purified by reversed-phase Hitachi HPLC (L-2455) on a Phenomenex Prodigy 10 μm ODS reversed-phase column (2.1 cm × 25 cm) using a gradient system to yield the linear capped Ac-PE(pY)LGLD and fluorescein-labeled F'-PE(pY)LGLD peptides, respectively. Similarly, other fluorescein-labeled peptides were synthesized according to this procedure.

**Ac-PE(pY)LGLD (shown here as PE(pY)LGLD)—MALDI-TOF (*m/z*)**

[C<sub>39</sub>H<sub>58</sub>N<sub>7</sub>NaO<sub>17</sub>P]: calcd [M + Na]<sup>+</sup>, 950.3524; found, 950.3524.

**F'-PE(pY)LGLD—MALDI-TOF (*m/z*)** [C<sub>58</sub>H<sub>67</sub>N<sub>7</sub>O<sub>22</sub>P]: calcd [M + H]<sup>+</sup>, 1244.4077; found, 1244.4080, [C<sub>58</sub>H<sub>66</sub>N<sub>7</sub>NaO<sub>22</sub>P]: calcd [M + Na]<sup>+</sup>, 1266.3896; found, 1266.3899.

**F'-G(pY)LPQTV—MALDI-TOF (*m/z*)** [C<sub>57</sub>H<sub>67</sub>N<sub>8</sub>NaO<sub>20</sub>P]: calcd [M + Na]<sup>+</sup>, 1237.4107; found, 1237.4108; [C<sub>57</sub>H<sub>67</sub>KN<sub>8</sub>O<sub>20</sub>P]: calcd [M + K]<sup>+</sup>, 1253.3846; found, 1253.3846.

**F'-NE(pY)TARQ—MALDI-TOF (*m/z*)** [C<sub>57</sub>H<sub>68</sub>N<sub>12</sub>O<sub>23</sub>P]: calcd [M + H]<sup>+</sup>, 1319.4258; found, 1319.4258.

**F'-AEEEEI(pY)GEFEAKKKK—MALDI-TOF (*m/z*)** [C<sub>102</sub>H<sub>139</sub>N<sub>19</sub>O<sub>36</sub>P]: calcd [M + H]<sup>+</sup>, 2236.9368; found, 2236.9370.

**F'-PS(pY)VNVQN-NH<sub>2</sub>—MALDI-TOF (*m/z*)** [C<sub>61</sub>H<sub>74</sub>N<sub>12</sub>O<sub>22</sub>P]: calcd [M + H]<sup>+</sup>, 1357.4778; found, 1357.4781.

**F'-G(pY)EEI—MALDI-TOF (*m/z*)** [C<sub>48</sub>H<sub>51</sub>N<sub>5</sub>O<sub>20</sub>P]: calcd [M + H]<sup>+</sup>, 1048.2865; found, 1048.2872.

### Cell Culture and Cytotoxicity Assay

**Cell Culture**—Human leukemia carcinoma cell line CCRF-CEM (ATCC no. CCL-119), ovarian adenocarcinoma SK-OV-3 (ATCC no. HTB-77), colorectal carcinoma HCT-116 (ATCC no. CCL-247), and normal human colon myofibroblast (CCD-18Co, ATCC no. CRL-1459) were obtained from American Type Culture Collection. Cells were grown on 75 cm<sup>2</sup> cell culture flasks with EMEM (Eagle's minimum essential medium), supplemented with 10% fetal bovine serum, and 1% penicillin/streptomycin solution (10,000 units of penicillin and 10 mg of streptomycin in 0.9% NaCl) in a humidified atmosphere of 5% CO<sub>2</sub>, 95% air at 37 °C.

**Flow Cytometry Studies**—Human leukemia adenocarcinoma (CCRF-CEM, 1 × 10<sup>7</sup> cells) or human ovarian adenocarcinoma cells (SK-OV-3, 3 × 10<sup>5</sup> cells) were taken in 6-well plates in opti-MEM or serum-free RPMI medium. Then the fluorescence-labeled phosphopeptides (F'-PE(pY)LGLD, F'-G(pY)LPQTV, F'-NE(pY)TARQ, F'-PS(pY)VNVQN-NH<sub>2</sub>, F'-AEEEEI(pY)GEFEAKKKK, or F'-G(pY)EEI) (5–10 μM) were added to the different wells containing [WR]<sub>4</sub> (25–50 μM) in media. The plates were

incubated for 1–2 h at 37 °C. Cells and fluorescence-labeled phosphopeptides alone were used as negative controls. After 1–2 h incubation, the media containing the peptide was removed. The cells were digested with 0.25% trypsin/ EDTA (0.53 mM) for 5 min to remove any artificial surface binding. Then the cells were washed twice with PBS. Finally, the cells were resuspended in flow cytometry buffer and analyzed by flow cytometry (FACSCalibur; Becton Dickinson) using FITC channel and CellQuest software. The data presented were based on the mean fluorescence signal for 10,000 cells collected. All assays were performed in triplicate. A similar procedure was used for linear (WR)<sub>4</sub> and linear tripodal peptide LPA<sub>4</sub> FACS studies.

**Cell Cytotoxicity Assay of [WR]<sub>4</sub> + PEpYLGLD Mixture**—SK-OV-3 (5,000 cells), CCRF-CEM (40,000 cells), HCT-116 (4,000), and CCD-18Co (3,000 cells) were seeded in 0.1 ml per well in 96-well plates 24 h prior to the experiment. The old medium (EMEM containing fetal bovine serum (FBS) (10%) for SK-OV-3, HCT-116 and CCD-18Co was removed. The stock solutions were prepared at high concentrations to generate maximum intermolecular interactions and then were diluted to desired concentrations for cellular studies. [WR]<sub>4</sub> (25 μM) + PEpYLGLD (5 μM) or [WR]<sub>4</sub> (50 μM) + PEpYLGLD (10 μM) in serum containing medium was added, and the cells were incubated for 24 h at 37 °C in a humidified atmosphere of 5% CO<sub>2</sub>. In case of CCRF-CEM (non-adherent cells), the final concentration was calculated after addition of the compounds. Cell viability was then determined by measuring the fluorescence intensity of the formazan product at 490 nm using a SpectraMax M2 microplate spectrophotometer. The percentage of cell survival was calculated as [(OD value of cells treated with the test mixture of compounds - OD value of culture medium)]/[(OD value of control cells - OD value of culture medium)] × 100%.

**Cellular Uptake Studies in the Presence of Inhibitors**—Human ovarian adenocarcinoma cells (SK-OV-3) were seeded in six well plates (3 × 10<sup>5</sup> cells/well) in opti-MEM. The cells were pre-incubated by various inhibitors including, nystatine (50 μg/ml), chloroquine (100 μM), chlorpromazine (30 μM), methyl-β-cyclodextrin (2.5 mM), and 5-(*N*-ethyl-*N*-isopropyl)amiloride (EIA, 50 μM) for 30 min. The treatment was removed, and the cells were incubated with [WR]<sub>4</sub> (25 μM), F'-PE(pY)LGLD (5 μM), and a similar concentration of inhibitors for 1 h. To induce ATP depletion, the cells were preincubated with 0.5% of 150 mM sodium azide in opti-MEM prior to the addition of the compound followed by 1 h incubation. Consequently, a similar FACS protocol was performed as described above.

**Confocal Microscopy on Live Cells**—Adherent SK-OV-3 cells were seeded with EMEM media overnight on coverslips in six well plates. Then the media were removed and washed with opti-MEM. The cells were treated with F'-PEpYLGLD (5 μM) in the presence or absence of [WR]<sub>4</sub> (25 μM) for 1 h at 37 °C. The stock solutions were prepared at high concentrations to generate maximum intermolecular interactions and then were diluted to desired concentrations for cellular studies. After 1 h incubation, the media containing the treatments were removed followed by washing with PBS three times. Then the coverslips were mounted on a microscope slide with mounting media with cells-attached side facing down. Laser scanning confocal microscopy was carried out using Carl Zeiss LSM 510 system. The cells were imaged using FITC and phase contrast channels.

**Transmission Electron Microscopy (TEM)**—TEM samples were prepared by drop casting of PEpYLGLD (1 mM in H<sub>2</sub>O), [WR]<sub>4</sub> (1 mM in H<sub>2</sub>O), or mixture of PEpYLGLD and [WR]<sub>4</sub> (1 mM in H<sub>2</sub>O) solution (incubated for one day) (10 μL) onto the formvar coated carbon grid of mesh size 300, which was allowed to sit for 2 min. Excess solvent was carefully removed by capillary action (filter paper). Grids were allowed to dry at room temperature for overnight. All images were taken using JEOL Transmission Electron



Microscope (Tokyo, Japan) maintained at 80 kv. After drop casting of peptide solutions, grids were then stained with uranyl acetate (20  $\mu$ L) for 2 min. Excess stain was removed, and the grids were allowed to dry overnight.

**Isothermal Titration Calorimetry (ITC)**—ITC was performed on a Microcal VP-ITC microcalorimeter (Microcal, Northampton, MA). Data acquisition and instrument control were carried out using a dedicated Origin software package. All the experiments were performed at 30 °C using cyclic peptide [WR]<sub>4</sub> (100  $\mu$ M) and PEPYLGLD (5 mM). Both PEPYLGLD and [WR]<sub>4</sub> were dissolved in water. Solution containing [WR]<sub>4</sub> (1.42 mL) was transferred into the sample cell. A solution of PEPYLGLD (5 mM, 10  $\mu$ L) was injected from the syringe (280  $\mu$ L) into the stirred sample cell (stirring speed 307 rpm). The reference cell was filled with deionized water. A 180 s time interval between injections was applied in order to allow the system to reach thermal equilibrium after each addition. Corrections were made for the dilution heat of the phosphopeptide, which was determined in control experiments under similar conditions. Analysis of the integrated heat data was performed using the Origin 7 package provided with the ITC instrument. Experimental data was fitted using a non-linear least-squares minimization algorithm to a theoretical titration curve. Different binding models were assumed, involving a single set of identical sites, two sets of independent sites, or sequential binding events. The equations were included in the commercial ITC Data analysis software package of Origin 7.0. The chi-square parameter  $\chi^2$  was used to establish the best fit.

**Circular Dichroism**—CD spectra were recorded on a JASCO J-810 spectropolarimeter using 1 mm path length cuvettes. The scan speed was 100 nm/min, and spectra were averaged over 8 scans. All experiments on the samples including [WR]<sub>4</sub> (25  $\mu$ M, H<sub>2</sub>O) and PEPYLGLD (25  $\mu$ M, H<sub>2</sub>O) were tested at room temperature. The CD for background reference (water) was measured and subtracted from the sample.

**Molecular Modeling**—Initial coordinates for [WR]<sub>5</sub> were obtained using GAUSSVIEW.<sup>32</sup> Ab initio Hartree Fock molecular orbital calculations with complete geometry optimizations were performed with 6–31G<sup>33</sup> basis set on monomer [WR]<sub>5</sub> utilizing GAUSSIAN'03 software. Geometry of monomers was completely optimized. All bond lengths, bond angles and dihedral angles were allowed to relax without any constraint.

## RESULTS AND DISCUSSION

### Chemistry

A number of fluorescence labeled phosphopeptides, F'-GpYLPQTV, F'-NEpYTARQ, F'-AEEEIYGEFEAKKKK, F'-PEpYLGLD, F'-pYVNVQN-NH<sub>2</sub>, and F'-GpYEEI, where F' is fluorescein, (Figure 1) were synthesized including according to the previously reported procedure.<sup>34</sup> These phosphopeptides were selected based on the sequence of phosphoprotein binding motif of protein tyrosine kinases that binds to the SH2 domain of other protein tyrosine kinases and leads to enzyme activation.<sup>35</sup>

As representative examples, the synthesis of Ac-PEpYLGLD (mentioned here as PEPYLGLD) and F'-PEpYLGLD is outlined here (Scheme 1). In general, the peptides were assembled on Wang resin using Fmoc solid-phase synthesis. Fmoc protection group at the N-terminal was removed. Subsequent capping reaction by acetic anhydride or conjugation reaction with 5(6)-carboxyfluorescein isobutyrate was performed in the presence of HOAt, PyAOP, and *N,N*-diisopropylethylamine (DIPEA) in DMF:DCM (5:1 v/v) followed by deprotection and cleavage from the resin in the presence of reagent R containing TFA/thioanisole/EDT/anisole (90:5:3:2 v/v/v/v) afforded crude products that were purified by

preparative reversed-phase HPLC. The structures of the compounds were confirmed by high-resolution MALDI TOF/TOF and/or high-resolution electrospray mass spectrometry. We have previously reported the synthesis of [WR]<sub>4</sub>.<sup>31</sup> A similar procedure was employed for the synthesis of other phosphopeptides by using appropriate resins and side chain protected amino acids.

### Cellular Uptake Studies

The cellular uptake of synthesized fluorescence-labeled phosphopeptides (10 μM) was examined in the presence and absence of [WR]<sub>4</sub> (50 μM) in human leukemia carcinoma (CCRF-CEM) cells after 2 h incubation at 37 °C using flow cytometry. After the incubation, cells were treated with trypsin to remove the cell surface-bound compound. [WR]<sub>4</sub> enhanced the cellular uptake of all phosphopeptides, including F'-GpYLPQTV, F'-NEpYTARQ, F'-AEEEEYGEFEAKKKK, F'-pYVNVQN-NH<sub>2</sub>, and F'-GpYEEI by 7-, 5-, 10-, 4-, and 19-fold, respectively. Fluorescence-activated cell sorting (FACS) analysis showed that the cellular uptake of F'-PEpYLGLD in the presence of [WR]<sub>4</sub> was increased dramatically by 27-fold when compared to F'-PEpYLGLD alone (Figure 2). These data indicate that the cellular uptake of the phosphopeptides was improved in the presence of [WR]<sub>4</sub> in a sequence dependent manner possibly due to different binding affinity between the phosphopeptides and [WR]<sub>4</sub>.

Because of dramatic effect of [WR]<sub>4</sub> on improving the cellular delivery of F'-PEpYLGLD, this phosphopeptide was selected for further studies. PEpYLGLD is a sequence that mimics the pTyr<sup>1246</sup> of ErbB2 that is responsible binding to the Chk SH2 domain.<sup>14</sup> The cellular uptake of F'-PEpYLGLD (10 μM) was also evaluated in the presence of the linear (WR)<sub>4</sub> (50 μM) using FACS under similar conditions and compared with that of cyclic [WR]<sub>4</sub> (Figure 3). The results showed that the linear (WR)<sub>4</sub> enhanced the cellular uptake of F'-PEpYLGLD by 17-fold in CCRF-CEM cells after 1 h incubation. However, the cyclic [WR]<sub>4</sub> was found to enhance the cellular uptake of F'-PEpYLGLD approximately 24-fold after 1 h incubation under similar conditions, suggesting the cyclic nature of the peptide is important for improving the cellular delivery of the phosphopeptide.

We have previously reported that Lys-(CH<sub>2</sub>)<sub>11</sub>-Arg-(CH<sub>2</sub>)<sub>11</sub>-Arg, a linear tripodal amphipathic peptide containing two arginine and one lysine residues (LPA4), enhanced the cellular delivery of a phosphopeptide (F'-GpYEEI) in the human breast carcinoma cells BT-20 (ATCC no. HTB-19) cells by 10-fold.<sup>30</sup> A comparative FACS study exhibited that the cellular uptake of F'-PEpYLGLD (10 μM) enhanced approximately 6 times in the presence of LP4 (50 μM) in CCRF-CEM cells after 1 h incubation. Thus, the transporting efficiency of LPA4 for F'-PEpYLGLD was significantly less than that of the cyclic [WR]<sub>4</sub> that showed 24-fold higher cellular delivery of the same phosphopeptide after 1 h incubation (Figure 3).

To evaluate the cytotoxicity of PEpYLGLD and [WR]<sub>4</sub>, cell viability assay was employed in three different cancer cell lines, including CCRF-CEM, SK-OV-3, human cologne carcinoma (HCT-116) cells, and normal human colon myofibroblast (CCD-18Co) cells at the experimental concentration of PEpYLGLD (5 μM) and [WR]<sub>4</sub> (25 μM). We have previously shown that cyclic [WR]<sub>4</sub> is not cytotoxic in HCT-116, CCRF-CEM, and SK-OV-3 cells at similar concentrations.<sup>31</sup> The mixture of [WR]<sub>4</sub> (25 μM) and PEpYLGLD (5 μM) or [WR]<sub>4</sub> (50 μM) and PEpYLGLD (10 μM) did not show any significant toxicity in normal cells and HCT-116 carcinoma cells after 24h incubation at 37 °C (Figure 4). While [WR]<sub>4</sub> (25 μM) and PEpYLGLD (5 μM) did not exhibit any cytotoxicity in SK-OV-3 and CCRF-CEM cells, the mixture showed 10–12% toxicity when higher concentrations of phosphopeptide (10 μM) and [WR]<sub>4</sub> (50 μM) were used. Thus, a concentration of

PEpYLGLD (5  $\mu\text{M}$ ) and [WR]<sub>4</sub> (25  $\mu\text{M}$ ) was used in SK-OV-3 and CCRF-CEM cells in all cellular uptake and confocal microscopy studies.

To investigate whether the performance of [WR]<sub>4</sub> is cell-type dependent, the intracellular uptake of a lower concentration of F'-PEpYLGLD (5  $\mu\text{M}$ ) was examined in human ovarian adenocarcinoma (SK-OV-3) cells in the presence or absence of [WR]<sub>4</sub> (25  $\mu\text{M}$ ). After 1 h incubation at 37 °C, FACS showed 22-fold higher fluorescence signals in the cells treated with F'-PEpYLGLD-loaded [WR]<sub>4</sub> compared to those treated with F'-PEpYLGLD alone, suggesting that the uptake of F'-PEpYLGLD is also enhanced by [WR]<sub>4</sub> in SK-OV-3 cells (Figure 5a).

The cellular uptake and internalization of many CPPs along with the conjugated cargo occurs predominantly via an endocytic pathway that involves macropinocytosis, caveolae pathway, clathrin-mediated endocytosis, or lipid-raft dependent endocytosis. The nature of the cell lines and the presence and type of the cargo could affect the specific mechanism employed by the CPP.<sup>36</sup> We have previously shown that the cellular uptake of [WR]<sub>4</sub> was independent of endocytosis.<sup>31a</sup> Thus, the mechanism of the cellular uptake of the complex mixture of [WR]<sub>4</sub> and F'-PEpYLGLD was evaluated in the presence of different inhibitors to determine whether the cargo changes the uptake mechanism.

To perform the ATP depletion, sodium azide was incubated with cells for 30 min prior to the incubation with the complex followed by 1 h incubation. Significant intracellular uptake of F'-PEpYLGLD in the presence of [WR]<sub>4</sub> in SK-OV-3 cells (Figure 5a) was still observed in the presence of sodium azide, suggesting that the cellular uptake is not significantly reduced by inducing ATP depletion.

Furthermore, [WR]<sub>4</sub> was still able to improve the cellular uptake of F'-PEpYLGLD in SK-OV-3 cells in the presence of different endocytic inhibitors, such as nystatin, EIA, chlorpromazine, chloroquine, and methyl  $\beta$ -cyclodextrin ruling out clathrin-mediated or caveolae-mediated endocytosis, and macropinocytosis as the major mechanism of uptake after 1 h incubation (Figure 5a). The cellular delivery of the phosphopeptide in the presence of [WR]<sub>4</sub> and inhibitors was still higher than F'-PEpYLGLD alone, suggesting the mechanism of cellular uptake is not exclusively endocytosis. This is a key advantage of [WR]<sub>4</sub> compared to known CPPs those are dependent on endocytotic entry. Another proposed mechanism for cellular uptake of CPPs is direct membrane transduction. The amphipathic nature of [WR]<sub>4</sub> and interactions of arginine and tryptophan residues in [WR]<sub>4</sub> with the corresponding negatively charged phospholipids and hydrophobic residues in lipid bilayer may have contributed to the initial entry into the cell membrane. Hydrophobic interactions between tryptophan residues and the lipids could lead to possible distortion of the outer phospholipid monolayer, followed by peptide internalization and enhanced cellular uptake of the cargo. Model studies have suggested that the direct transduction occurs through carpet-like perturbations, pore formation, or inverted micelles formed in the bilayer membrane.<sup>36</sup> Further mechanistic studies will provide insights for designing the next generation of cyclic peptides as molecular transporters of phosphopeptides.

The cellular uptake of F'-PEpYLGLD was found to be rapid and time-dependent. F'-PEpYLGLD (5  $\mu\text{M}$ ) was incubated with [WR]<sub>4</sub> (25  $\mu\text{M}$ ) at different incubation times including 10 min, 30 min, and 1 h. FACS results showed that the cellular uptake of F'-PEpYLGLD was increased in a time-dependent pattern (Figure 5b). On the other hand, the cellular uptake of F'-PEpYLGLD was not changed significantly in the absence of [WR]<sub>4</sub>.

Confocal microscopy in live cells was used to monitor the cellular uptake of F'-PEpYLGLD in the presence and absence of the peptide. Incubation of mixture of F'-PEpYLGLD [WR]<sub>4</sub> showed significantly higher cellular uptake when compared to that of F'-PEpYLGLD alone



as shown by intracellular fluorescence. Comparison of the intracellular localization of F'-PEpYLGLD-loaded [WR]<sub>4</sub> to F'-PEpYLGLD alone after 1 h incubation at 37 °C confirmed that the presence of the cyclic peptide is critical for the enhanced cellular permeability (Figure 6).

Circular dichroism (CD), Transmission electron microscopy (TEM), and Isothermal Titration Calorimetry (ITC) were used to gain a better insight about the interaction of [WR]<sub>4</sub> and PEpYLGLD. CD was used to get a better understanding of the secondary structure change in [WR]<sub>4</sub> and PEpYLGLD upon mixing and intermolecular interactions. All spectra were corrected for background by subtraction of the blank. CD results showed that PEpYLGLD (25 μM) loaded with [WR]<sub>4</sub> (25 μM) showed a different CD pattern compared to those of parent analogues, [WR]<sub>4</sub> (25 μM) and PEpYLGLD (25 μM). While PEpYLGLD did not show any specific structure, both PEpYLGLD loaded [WR]<sub>4</sub> and [WR]<sub>4</sub> exhibited a maxima at 230 nm and a minima at 203–205 nm, suggesting that [WR]<sub>4</sub> maintain the secondary structure partially upon binding with in PEpYLGLD. These secondary structures are distinct from known α and β structures. However, the pattern of the spectra shows some major differences between PEpYLGLD-loaded [WR]<sub>4</sub> and [WR]<sub>4</sub> at <190 nm and in intensity of ellipticity in maxima and minima peaks (Figure 7).

The interaction between PEpYLGLD and [WR]<sub>4</sub> was visualized by using TEM. The stable mixture of [WR]<sub>4</sub> and PEpYLGLD was prepared at a high concentration to achieve the maximum interaction. An optimized balance between the hydrophobic and electrostatic interactions generated by the drug and the carrier led to the formation of nanosized particles. [WR]<sub>4</sub> generated self-assembled nanostructures after one day incubation at room temperature. Initial TEM imaging of negatively stained [WR]<sub>4</sub> (1 mM aqueous solution) showed circular vesicle-like structures with approximate size of 25–60 nm. TEM images of PEpYLGLD (Figure 8a) exhibited amorphous structures with approximate size of 40 nm. When PEpYLGLD was added to [WR]<sub>4</sub> in solution, PEpYLGLD-loaded [WR]<sub>4</sub> formed some larger noncircular nanosized structures with approximate width and height of 125 nm and 60 nm, respectively, possibly through electrostatic and/or hydrophobic intermolecular interactions between the positively charged cyclic peptide and negatively charged phosphopeptide (Figure 8b). TEM images further confirm that the structures of [WR]<sub>4</sub> modifies upon binding with PEpYLGLD, generating new nanostructures.

ITC was used to measure the binding constants between PEpYLGLD and [WR]<sub>4</sub> in complex formation. The ITC measurements were carried out at 30 °C by adding an aqueous solution PEpYLGLD (6 mM) to [WR]<sub>4</sub> (500 μM) solution in water. The equation for three sequential binding events was found to be the best fit for the data as shown by the Origin software. The chi squared  $\chi^2$  value was found  $1.6 \times 10^2$  produced by three sequential models. The binding constants values for three sequential events were determined  $K_1 = 7.1 \times 10^3 \text{ M}^{-1}$ ,  $K_2 = 4.9 \times 10^3 \text{ M}^{-1}$ , and  $K_3 = 1.1 \times 10^4 \text{ M}^{-1}$  (Figure 9). The enthalpies ( $\Delta H$ ) for the binding were -0.17, 0.30, and -0.23 kcal/mol, and the entropies ( $T\Delta S$ ) were 5.2, 5.4, and 5.3 kcal/mol, respectively. Therefore, the Gibbs free energies ( $\Delta G$ ) calculated from  $\Delta H$  and  $T\Delta S$  were -5.4, -5.1, and -5.6 kcal/mol for each binding site. ITC data suggest that PEpYLGLD and [WR]<sub>4</sub> form a complex through multistep intermolecular interactions including hydrophobic interactions driven by entropy as shown previously.<sup>37</sup> These data indicate that in addition to the electrostatic interactions between positively charged cyclic peptide and negatively charged phosphopeptide, hydrophobic forces also contribute in the complex formation possibly due to the interactions of the hydrophobic tryptophan and leucine residues in [WR]<sub>4</sub> and PEpYLGLD, respectively. ITC and TEM results are relevant with cellular studies since the stock solutions were prepared at high concentrations to generate maximum intermolecular interactions and then were diluted further to obtain desired concentration for cell-based assays.

Molecular modeling studies of [WR]<sub>5</sub>, a similar model cyclic peptide, were used to gain better insights of three dimensional structure of this class of peptides. Initial coordinates for [WR]<sub>5</sub> were obtained followed by Ab initio Hartree Fock molecular orbital calculations with complete geometry optimizations utilizing GAUSSIAN'03 software.<sup>32</sup> Two different conformations were obtained (Figure 10). The lowest energy conformation did not allow any intramolecular H-bonding. Higher energy conformation (25 kCal/mol) showed intramolecular H-bonding between cationic and neutral side chains. Side chains have to reorganize for efficient intramolecular H-bonding resulting in higher energy conformation. In the lowest energy conformation tryptophan side chains are disposed perpendicular to backbone. Higher energy conformation being more planar seems more suited for stacking.

## Conclusions

In summary, a new carrier system for the delivery of cell impermeable phosphopeptides was discovered using cyclic octapeptide [WR]<sub>4</sub> containing alternative tryptophan and arginine residues. The cellular uptake of F'-PEpYLGLD was enhanced by 27-fold in the presence of [WR]<sub>4</sub>, and was found to be time-dependent. Positively charged cyclic peptide formed nanostructures in the presence of negatively charged PEpYLGLD as shown by TEM. Binding affinity between [WR]<sub>4</sub> and PEpYLGLD was further confirmed by ITC studies. To the best of our knowledge, this is the first report of using cyclic peptides for noncovalent cellular delivery of cell impermeable phosphopeptides. These data provide insights about using cell penetrating cyclic peptides as PAs for delivery of negatively charged cell impermeable phosphopeptides.

## Supplementary Material

Refer to Web version on PubMed Central for supplementary material.

## Acknowledgments

We acknowledge the financial support from National Science Foundation, Grant Number CHE 0748555. We thank the National Institute of General Medical Sciences of the National Institutes of Health under grant number 8 P20 GM103430-12 for sponsoring the core facility.

## ABBREVIATIONS

<b>BT-20</b>	human breast carcinoma cell line
<b>CCRF-CEM</b>	human leukemia carcinoma cell line
<b>CD</b>	Circular dichroism
<b>CCD-18Co</b>	normal human colon myofibroblast
<b>CPPs</b>	Cell-Penetrating Peptides
<b>DCM</b>	dichloromethane
<b>DIPEA</b>	<i>N,N</i> -diisopropylethylamine
<b>DMF</b>	<i>N,N</i> -dimethylformamide
<b>EIA</b>	5-( <i>N</i> -ethyl- <i>N</i> -isopropyl)amiloride
<b>F'</b>	fluorescein
<b>FACS</b>	Fluorescence Activated Cell Sorter
<b>FBS</b>	fetal bovine serum

<b>DCM</b>	dichloromethane
<b>EDT</b>	ethandithiol
<b>HBTU</b>	2-(1 <i>H</i> -benzotriazole-1-yl)-1,1,3,3-tetramethyluronium hexafluorophosphate
<b>HCT-116</b>	human colorectal carcinoma
<b>HOBt</b>	hydroxybenzotriazole
<b>HOAt</b>	1-hydroxy-7-azabenzotriazole
<b>ITC</b>	Isothermal Calorimetric
<b>NMM</b>	<i>N</i> -methylmorpholine
<b>PAs</b>	Peptide amphiphiles
<b>PTB</b>	phosphotyrosine binding
<b>PyAOP</b>	7-azabenzotriazol-1-yloxy tripyrrolidinophosphonium hexafluorophosphate)
<b>SH2</b>	Src homology 2
<b>SK-OV-3</b>	human ovarian adenocarcinoma
<b>TFA</b>	trifluoroacetic acid
<b>TEM</b>	Transmission Electron Microscopy

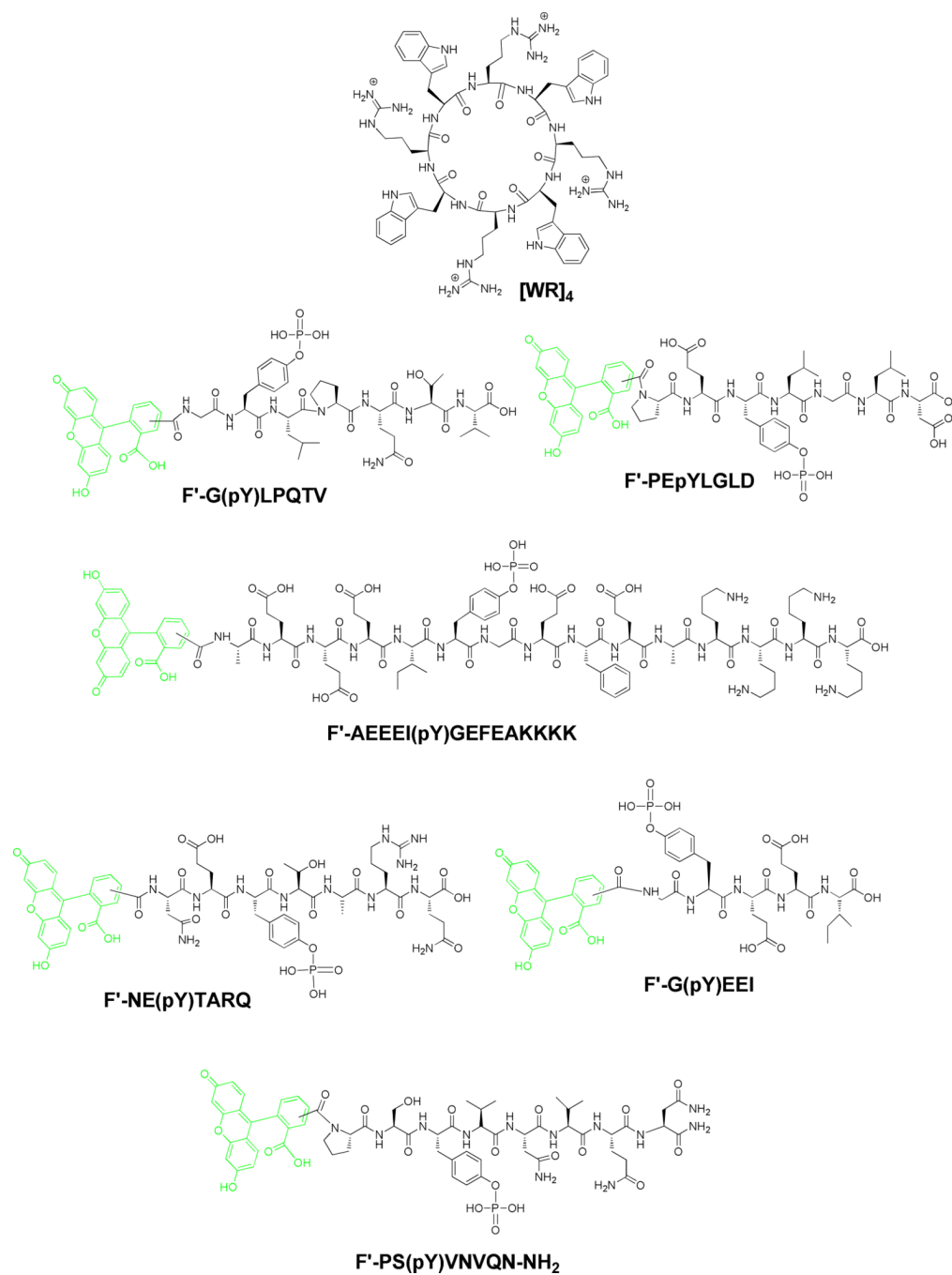
## REFERENCES

1. Bulut S, Erkal TS, Toksoz S, Tekinay AB, Tekinay T, Guler MO. Slow release and delivery of antisense oligonucleotide drug by self-assembled peptide amphiphile nanofibers. *Biomacromolecules*. 2011; 12:3007–3014. [PubMed: 21707109]
2. Kim JK, Anderson J, Jun HW, Repka MA, Jo S. Self-assembling peptide amphiphile-based nanofiber gel for bioresponsive cisplatin delivery. *Mol. Pharm.* 2009; 6:978–985. [PubMed: 19281184]
3. Dheur S, Dias N, Van Aerschot A, Herdewijn P, Bettinger T, Rémy JS, Hélène C, Saison-Behmoaras ET. Polyethylenimine but not cationic lipid improves antisense activity of 3'-capped phosphodiester oligonucleotides. *Antisense Nucleic Acid Drug Dev.* 1999; 9:515–525. [PubMed: 10645777]
4. Jeong JH, Kim SH, Kim SW, Park TG. Intracellular delivery of poly(ethylene glycol) conjugated antisense oligonucleotide using cationic lipids by formation of self-assembled polyelectrolyte complex micelles. *J. Nanosci. Nanotechnol.* 2006; 6:2790–2795. [PubMed: 17048484]
5. Crombez L, Aldrian-Herrada G, Konate K, Nguyen GN, McMaster GK, Bresseur R, Heitz GK, Divita GA. new potent secondary amphipathic cell-penetrating peptide for siRNA delivery into mammalian cells. *Molecular Therapy*. 2008; 17:95–103. [PubMed: 18957965]
6. El-Andaloussi S, Holm T, Langel U. Cell-penetrating peptides: mechanisms and applications. *Curr. Pharm. Des.* 2005; 11:3597–3611. [PubMed: 16305497]
7. Fotin-Mleczek M, Fischer R, Brock R. Endocytosis and cationic cell-penetrating peptides--a merger of concepts and methods. *Curr. Pharm. Des.* 2005; 11:3613–3628. [PubMed: 16305498]
8. Fernandez-Carneado J, Kogan MJ, Pujals S, Giralt E. Amphipathic peptides and drug delivery. *Biopolymers*. 2004; 76:196–203. [PubMed: 15054899]
9. Deshayes S, Morris MC, Divita G, Heitz F. Cell-penetrating peptides: tools for intracellular delivery of therapeutics. *Cell. Mol. Life Sci.* 2005; 62:1839–1849. [PubMed: 15968462]

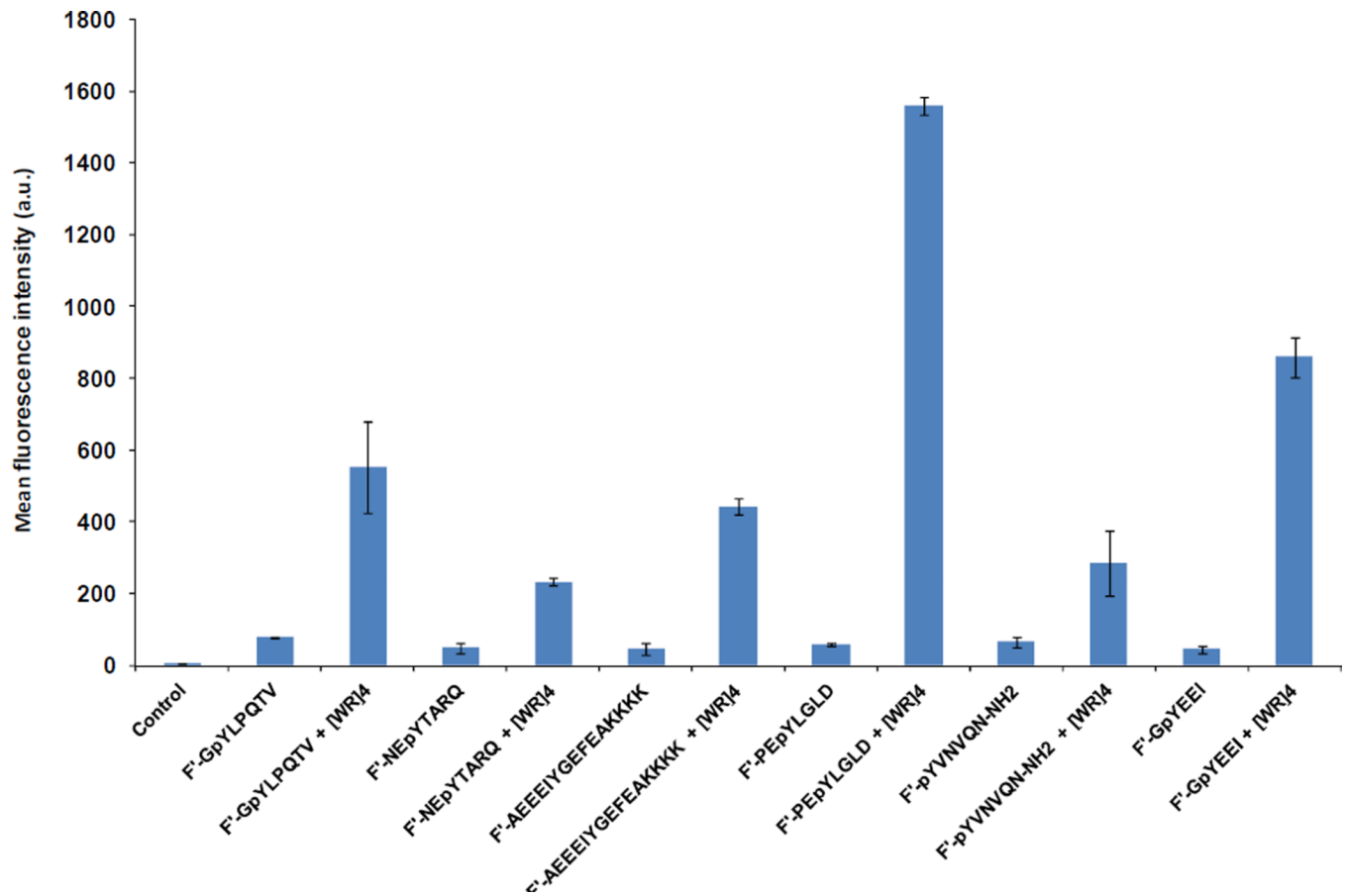
10. Torchilin VP, Rammohan R, Weissig V, Levchenko TS. TAT peptide on the surface of liposomes affords their efficient intracellular delivery even at low temperature and in the presence of metabolic inhibitors. *Proc. Natl. Acad. Sci. USA.* 2001; 98:8786–8791. [PubMed: 11438707]
11. Silhol M, Tyagi M, Giacca M, Lebleu B, Vives E. Different mechanisms for cellular internalization of the HIV-1 Tat-derived cell penetrating peptide and recombinant proteins fused to Tat. *Eur. J. Biochem.* 2002; 269:494–501. [PubMed: 11856307]
12. Thorén PE, Persson D, Isakson P, Goksör M, Onfelt A, Nordén B. Uptake of analogs of penetratin, Tat(48–60) and oligoarginine in live cells. *Biochem. Biophys. Res. Commun.* 2003; 307:100–107. [PubMed: 12849987]
13. Zhou Y, Abagyan R. How and why phosphotyrosine-containing peptides bind to the SH2 and PTB domains. *Folding Des.* 1998; 3:513–522.
14. Machida K, Mayer BJ. The SH2 domain: versatile signaling module and pharmaceutical target. *Biochim. Biophys. Acta.* 2005; 1747:1–25. [PubMed: 15680235]
15. Songyang Z, Shoelson SE, Chaudhuri M, Gish G, Pawson T, Haser WG, King F, Roberts T, Ratnofsky S, Lechleider RJ, Neel BG, Birge RB, Fajardo JE, Chou MM, Hanafusa H, Schaffhausen B, Cantley LC. SH2 domains recognize specific phosphopeptide sequences. *Cell.* 1993; 72:767–778. [PubMed: 7680959]
16. Pinna LA, Donella-Deana A. Phosphorylated synthetic peptides as tools for studying protein phosphatases. *Biochim. Biophys. Acta.* 1994; 1222:415–431. [PubMed: 8038211]
17. Ottinger EA, Shekels LL, Bernlohr DA, Barany G. Synthesis of phosphotyrosine-containing peptides and their use as substrates for protein tyrosine phosphatases. *Biochemistry.* 1993; 32:4354–4361. [PubMed: 7682846]
18. Burke TR, Yao ZJ, Liu DG, Voigt J, Gao Y. Phosphoryltyrosyl mimetics in the design of peptide-based signal transduction inhibitors. *Biopolymers.* 2001; 60:32–44. [PubMed: 11376431]
19. Eck MJ. A new flavor in phosphotyrosine recognition. *Structure.* 1995; 3:421–424. [PubMed: 7545066]
20. Dunican DJ, Doherty P. Designing cell-permeant phosphopeptides to modulate intracellular signaling pathways. *Biopolymers.* 2001; 60:45–60. [PubMed: 11376432]
21. Williams EJ, Dunican DJ, Green PJ, Howell FV, Derossi D, Walsh FS, Doherty P. Selective inhibition of growth factor-stimulated mitogenesis by a cell-permeable Grb2-binding peptide. *J. Biol. Chem.* 1997; 272:22349–22354. [PubMed: 9268386]
22. Derossi D, Williams EJ, Green PJ, Dunican DJ, Doherty P. Stimulation of mitogenesis by a cell-permeable PI 3-kinase binding peptide. *Biochem. Biophys. Res. Commun.* 1998; 251:148–152. [PubMed: 9790922]
23. Theodore L, Derossi D, Chassaing G, Llirbat B, Kubes M, Jordan P, Chneiweiss H, Godement P, Prochiantz A. Intraneuronal delivery of protein kinase C pseudosubstrate leads to growth cone collapse. *J. Neurosci.* 1995; 15:7158–7167. [PubMed: 7472470]
24. Garrido-Hernandez H, Moon KD, Geahlen RL, Borch RF. Design and synthesis of phosphotyrosine peptidomimetic prodrugs. *J. Med. Chem.* 2006; 49:3368–3376. [PubMed: 16722656]
25. Boutselis IG, Yu X, Zhang ZY, Borch RF. Synthesis and cell-based activity of a potent and selective protein tyrosine phosphatase 1B inhibitor prodrug. *J. Med. Chem.* 2007; 50:856–864. [PubMed: 17249650]
26. Arrendale A, Kim K, Choi JY, Li W, Geahlen RL, Borch RF. Synthesis of a phosphoserine mimetic prodrug with potent 14-3-3 protein inhibitory activity. *Chem. Biol.* 2012; 19:764–771. [PubMed: 22726690]
27. Panigrahi K, Nelson DL, Berkowitz DB. Unleashing a "true" pSer-mimic in the cell. *Chem. Biol.* 2012; 19:666–667. [PubMed: 22726679]
28. Tarrant MK, Rho HS, Xie Z, Jiang YL, Gross C, Culhane JC, Yan G, Qian J, Ichikawa Y, Matsuoka T, Zachara N, Etkorn FA, Hart GW, Jeong JS, Blackshaw S, Zhu H, Cole PA. Regulation of CK2 by phosphorylation and O-GlcNAcylation revealed by semisynthesis. *Nat. Chem. Biol.* 2012; 8:262–269. [PubMed: 22267120]

29. Goguen BN, Hoffman BD, Sellers JR, Schwartz MA, Imperiali B. Light-triggered myosin activation for probing dynamic cellular processes. *Angew. Chem. Int. Ed. Engl.* 2011; 50:5667–5670. [PubMed: 21542072]
30. Ye G, Nam NH, Kumar A, Saleh A, Shenoy DB, Amiji MM, Lin X, Sun G, Parang K. Synthesis and evaluation of tripodal peptide analogues for cellular delivery of phosphopeptides. *J. Med. Chem.* 2007; 50:3604–3617. [PubMed: 17580848]
31. (a) Mandal D, Nasrolahi Shirazi A, Parang K. Cell-penetrating homochiral cyclic peptides as nuclear-targeting molecular transporters. *Angew. Chem. Int. Ed.* 2011; 50:9633–9637. (b) Nasrolahi Shirazi A, Tiwari RK, Chhikara BS, Mandal D, Parang K. Design and evaluation of cell-penetrating peptide-doxorubicin conjugates as prodrugs. *Molecular Pharmaceutics.* 2013; 10:488–499. [PubMed: 23301519]
32. Dennington, R., II; Keith, T.; Millan, J.; Eppinnett, K.; Hovell, WL.; Gilliland, R. Gaussview, Version 3.09. Semichem Inc, S., Mission KS; 2003.
33. Ditchfield R, Hehre WJ, Pople JA. An Extended Gaussian-Type Basis for Molecular-Orbital Studies of Organic Molecules. *J. Chem. Phys.* 1971; 54:724–728.
34. Nam NH, Ye G, Sun G, Parang K. Conformationally constrained peptide analogues of pTyr-Glu-Glu-Ile as inhibitors of the Src SH2 domain binding. *J. Med. Chem.* 2004; 47:3131–3141. [PubMed: 15163193]
35. (a) Sawyer TK. Biopoly Src homology-2 domains: structure, mechanisms, and drug discovery. *Pep. sci.* 1998; 47:243–261. (b) Vu CB, Corpuz EG, Pradeepan SG, Violette S, Bartlett C, Sawyer TK. Bioorg. Nonpeptidic SH2 inhibitors of the tyrosine kinase ZAP-70. *Med. Chem. Lett.* 1999; 9:3009–3014. (c) Vu CB. Recent advances in the design and synthesis of SH2 inhibitors of Src, Grb2 and ZAP-70. *Curr. Med. Chem.* 2000; 7:1081–1100. [PubMed: 10911019] (d) Muller G. Peptidomimetics SH2 domain antagonists for targeting signal transduction. *Topics Curr. Chem.* 2000; 211:17–59. (e) Vu CB, Corpuz EG, Merry TJ, Pradeepan SG, Bartlett C, Bohacek RS, Botfield MC, Eyermann CJ, Lynch BA, MacNeil IA, Ram MK, van Schravendijk MR, Violette S, Sawyer TK. Discovery of potent and selective SH2 inhibitors of the tyrosine kinase ZAP-70. *J. Med. Chem.* 1999; 42:4088–4098. [PubMed: 10514279] (f) Cody WL, Lin Z, Panek RL, Rose DW, Rubin JR. Progress in the development of inhibitors of SH2 domains. *Curr. Pharm. Des.* 2000; 6:59–98. [PubMed: 10637372]
36. Madani F, Lindberg S, Langel U, Futaki S, Gräslund A. Mechanisms of cellular uptake of cell-penetrating peptides. *J. Biophys.* 2011; 2011:414729. [PubMed: 21687343]
37. (a) Ball V, Maechling C. Isothermal microcalorimetry to investigate non specific interactions in biophysical chemistry. *Int. J. Mol. Sci.* 2009; 10:3283–3315. [PubMed: 20111693] (b) Bouchemal K. New challenges for pharmaceutical formulations and drug delivery systems characterization using isothermal titration calorimetry. *Drug. Discov. Today.* 2008; 13:960–972. [PubMed: 18617012]

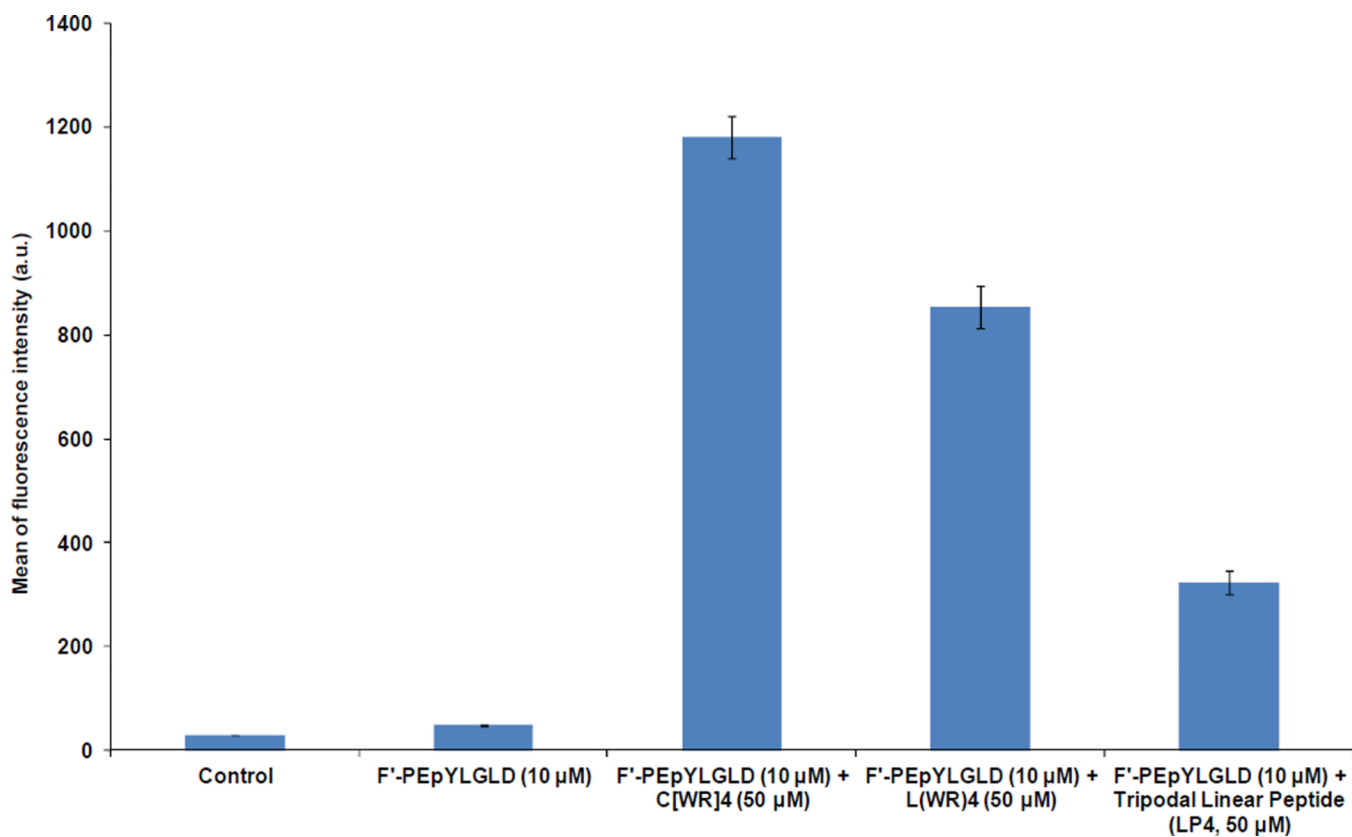




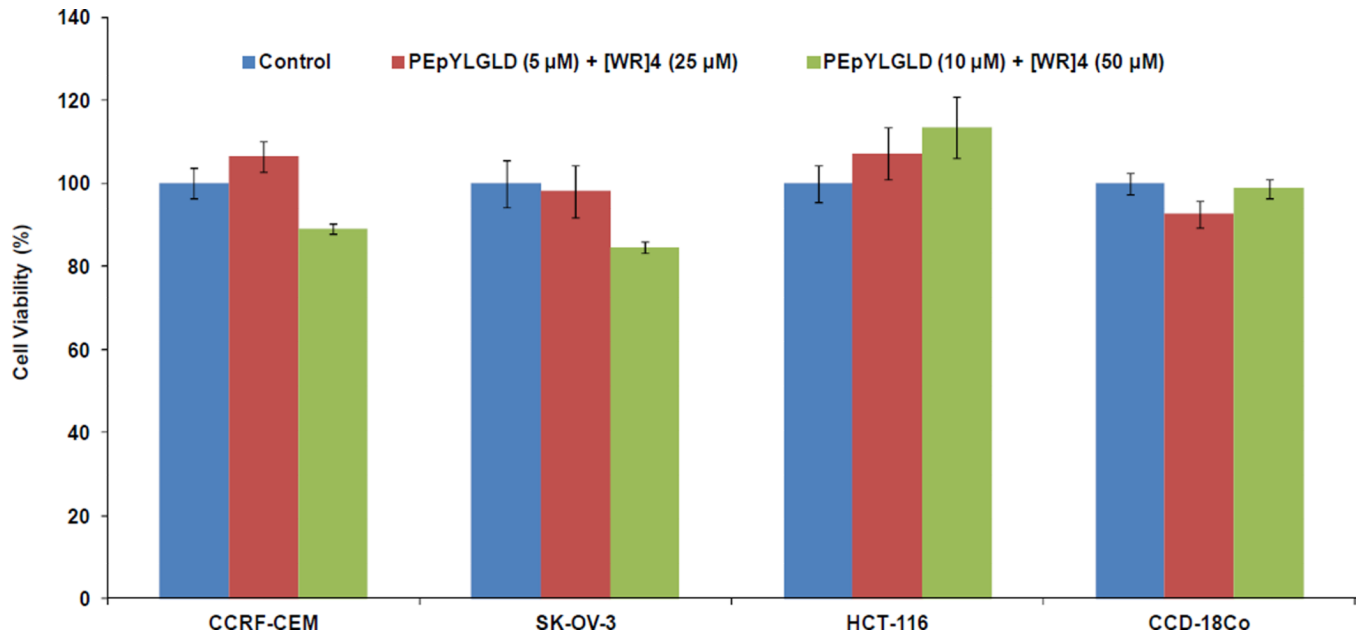
**Figure 1.**  
Chemical structure of [WR]<sub>4</sub> and phosphopeptides synthesized by Fmoc-based peptide chemistry.



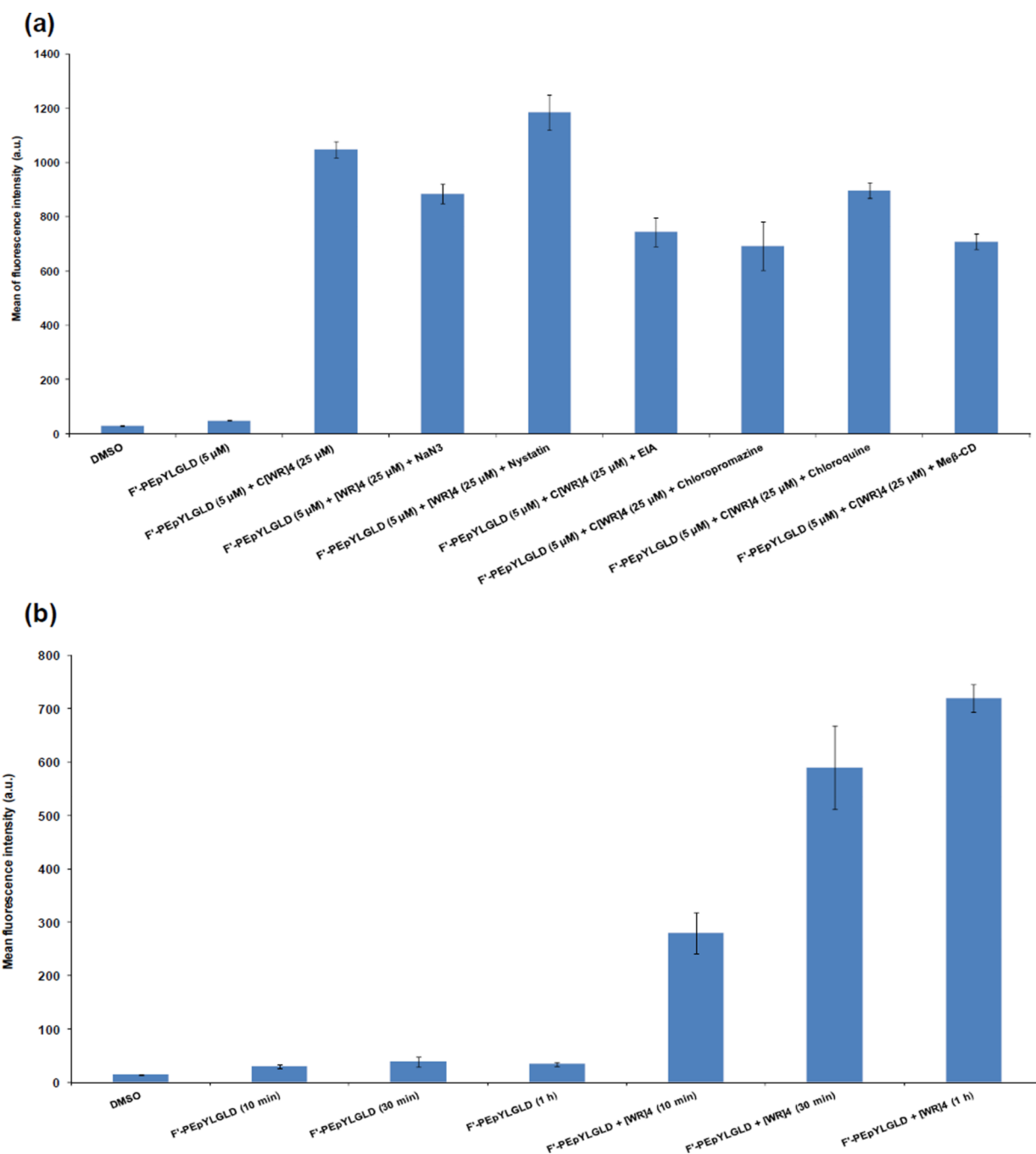
**Figure 2.** Comparative cellular uptake of F'-phosphopeptides (10  $\mu$ M) in the presence of [WR]<sub>4</sub> (50  $\mu$ M) in CCRF-CEM cells after 2 h.



**Figure 3.** Cellular uptake of F'-PEpYLGLD (10 μM) in the presence of cyclic [WR]<sub>4</sub> (50 μM), linear (WR)<sub>4</sub> (50 μM), or a tripodal linear peptide (LP4) (50 μM) in CCRF-CEM cells after 1 h incubation.

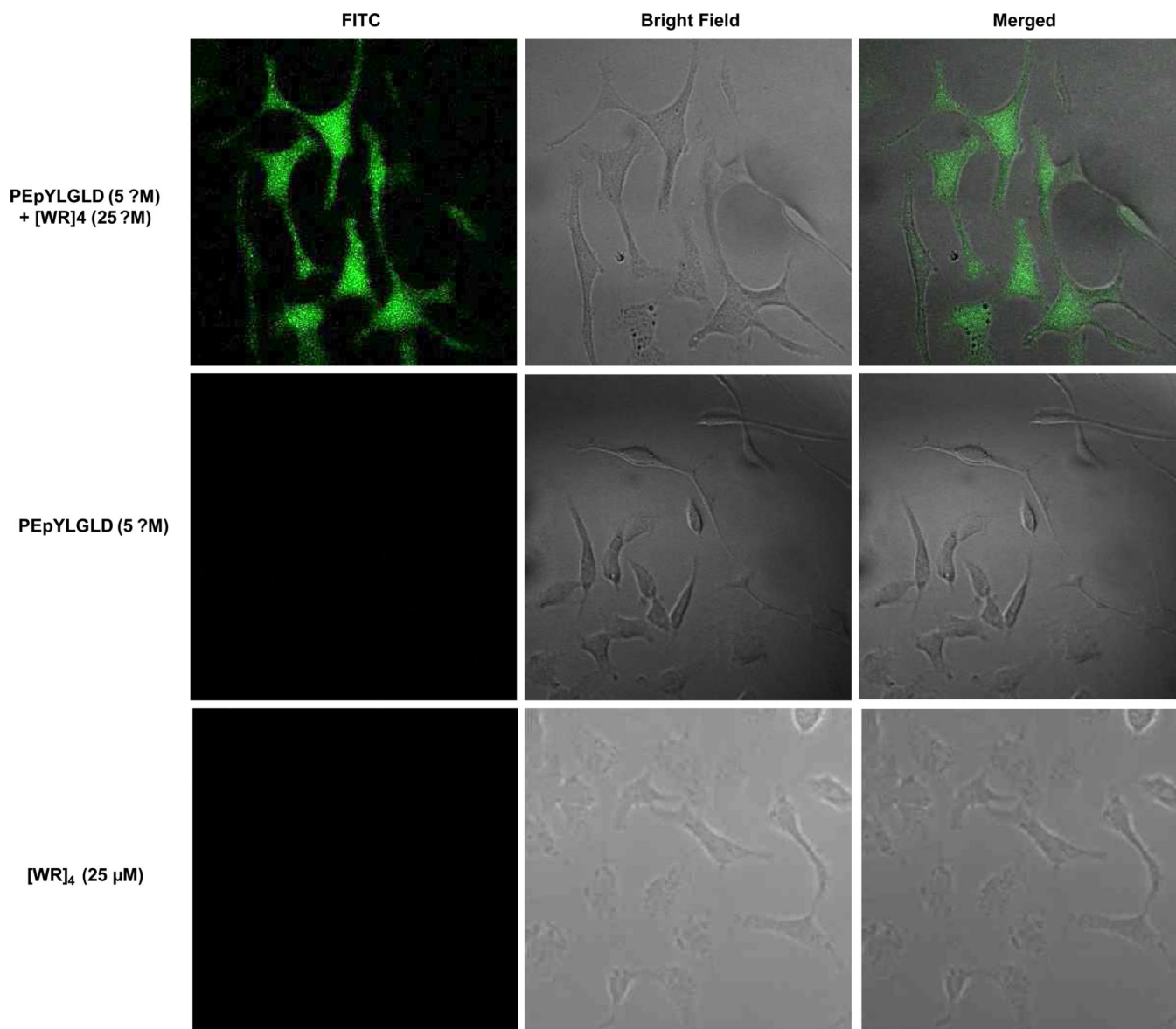


**Figure 4.** Cytotoxicity assay of the mixture of PEpYLGLD (5 and 10  $\mu\text{M}$ ) and [WR]<sub>4</sub> (25 and 50  $\mu\text{M}$ ) in CCRF-CEM, HCT-116, SK-OV-3, and CCD-18Co cells after 24 h.

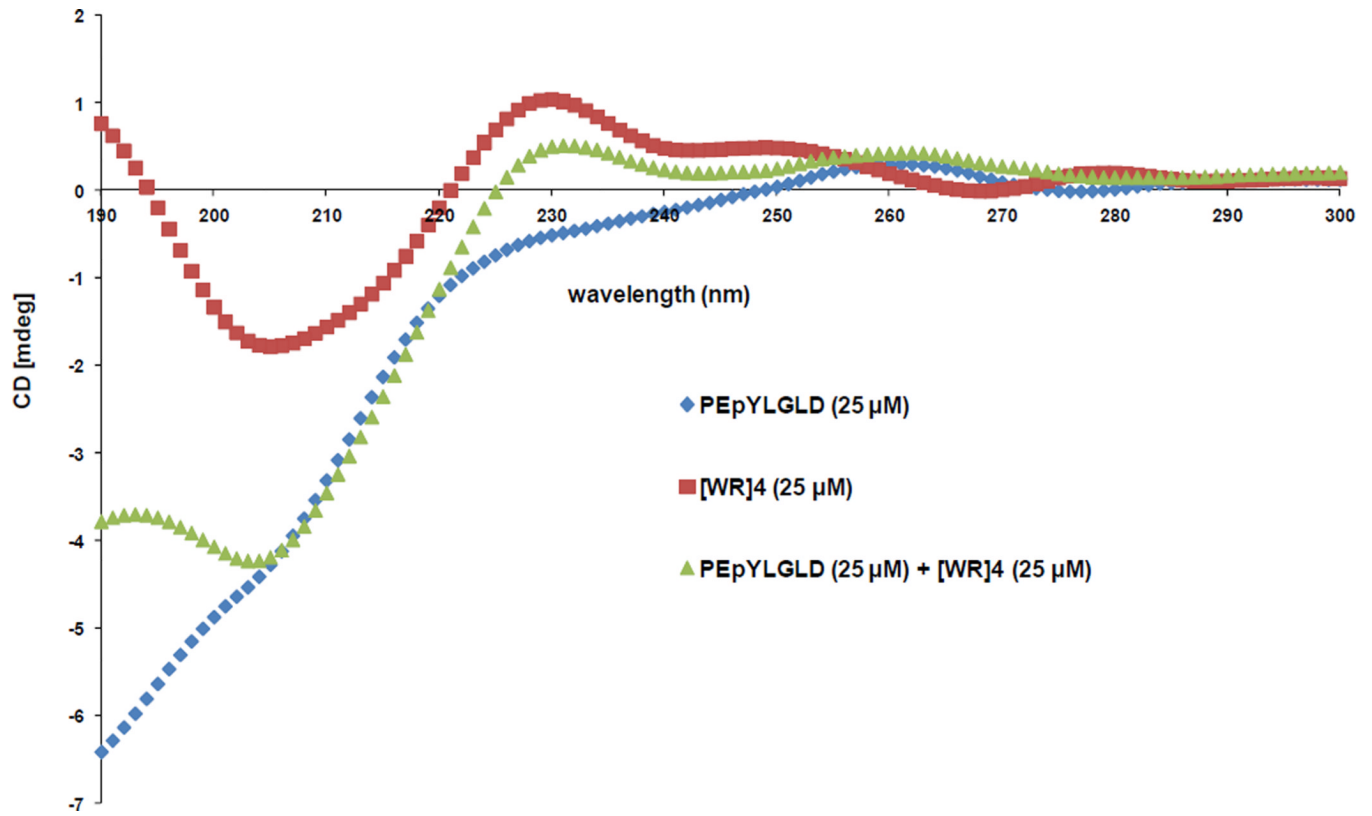
**Figure 5.**

(a) Cellular uptake of F'-PEpYLGLD (5 μM) + WR]4 (25 μM) in the absence or presence of different endocytic inhibitors and sodium azide in SK-OV-3 cells after 1 h; (b) FACS analysis of cellular uptake assays of F'-PEpYLGLD (5 μM)-loaded [WR]4 (25 μM) compared to F'-PEpYLGLD (5 μM) alone in CCRF-CEM.

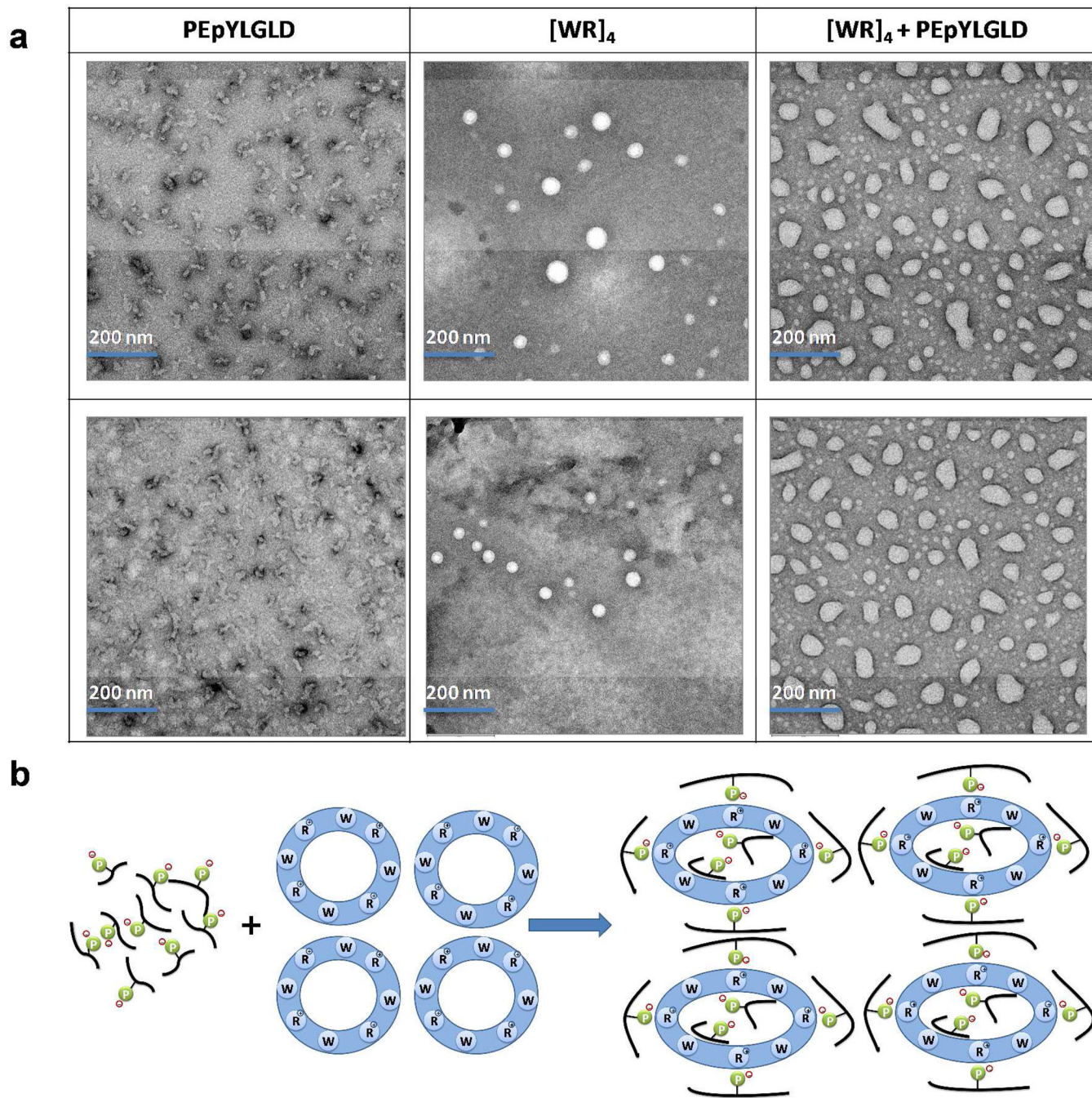




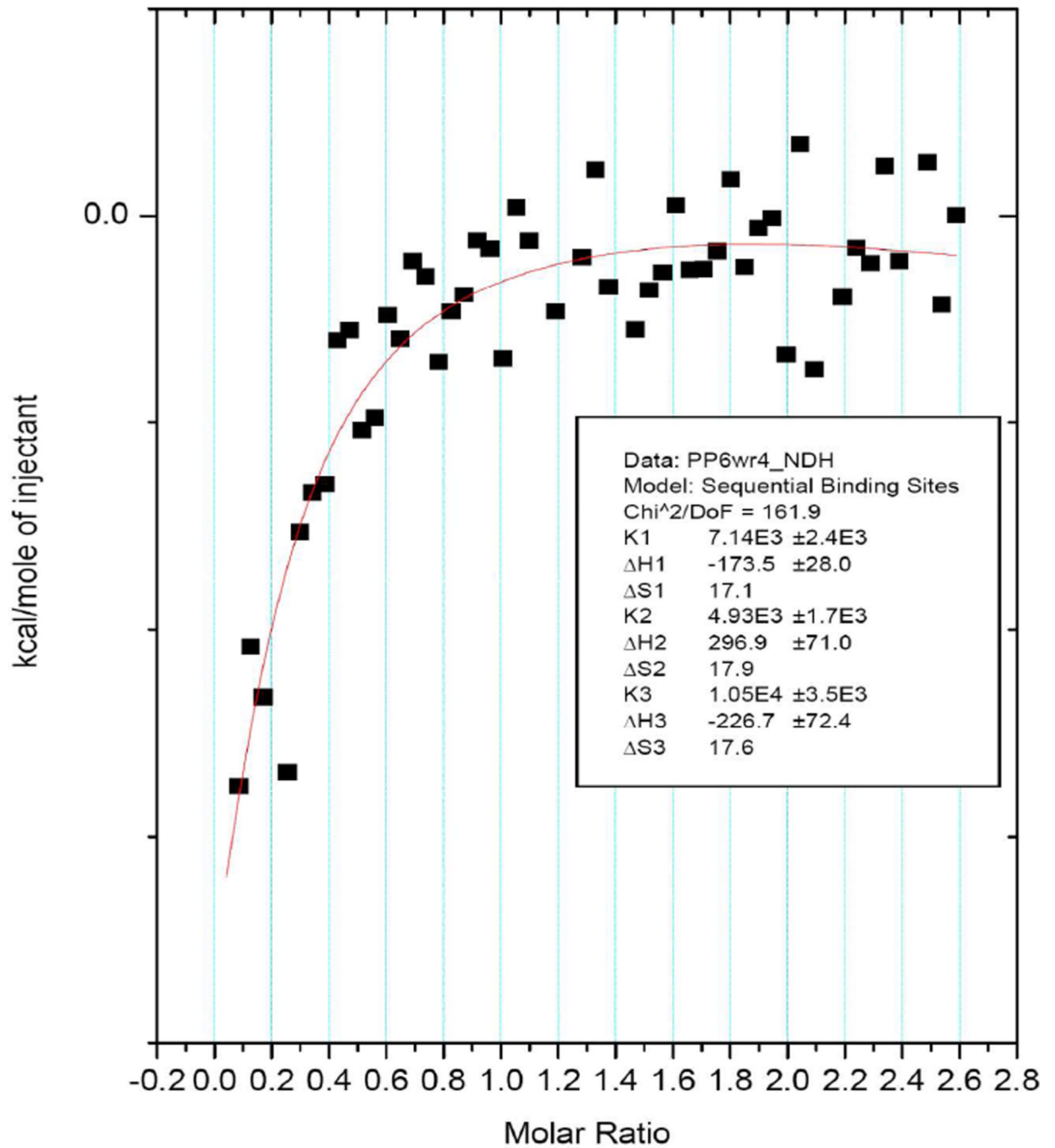
**Figure 6.** Confocal microscope images of F'-PEpYLGLD (5  $\mu$ M) uptake by SK-OV-3 cells in the presence of [WR]<sub>4</sub> (25  $\mu$ M).



**Figure 7.**  
CD pattern of PEpYLGLD and [WR]<sub>4</sub> compared to the PEpYLGLD-loaded [WR]<sub>4</sub>.

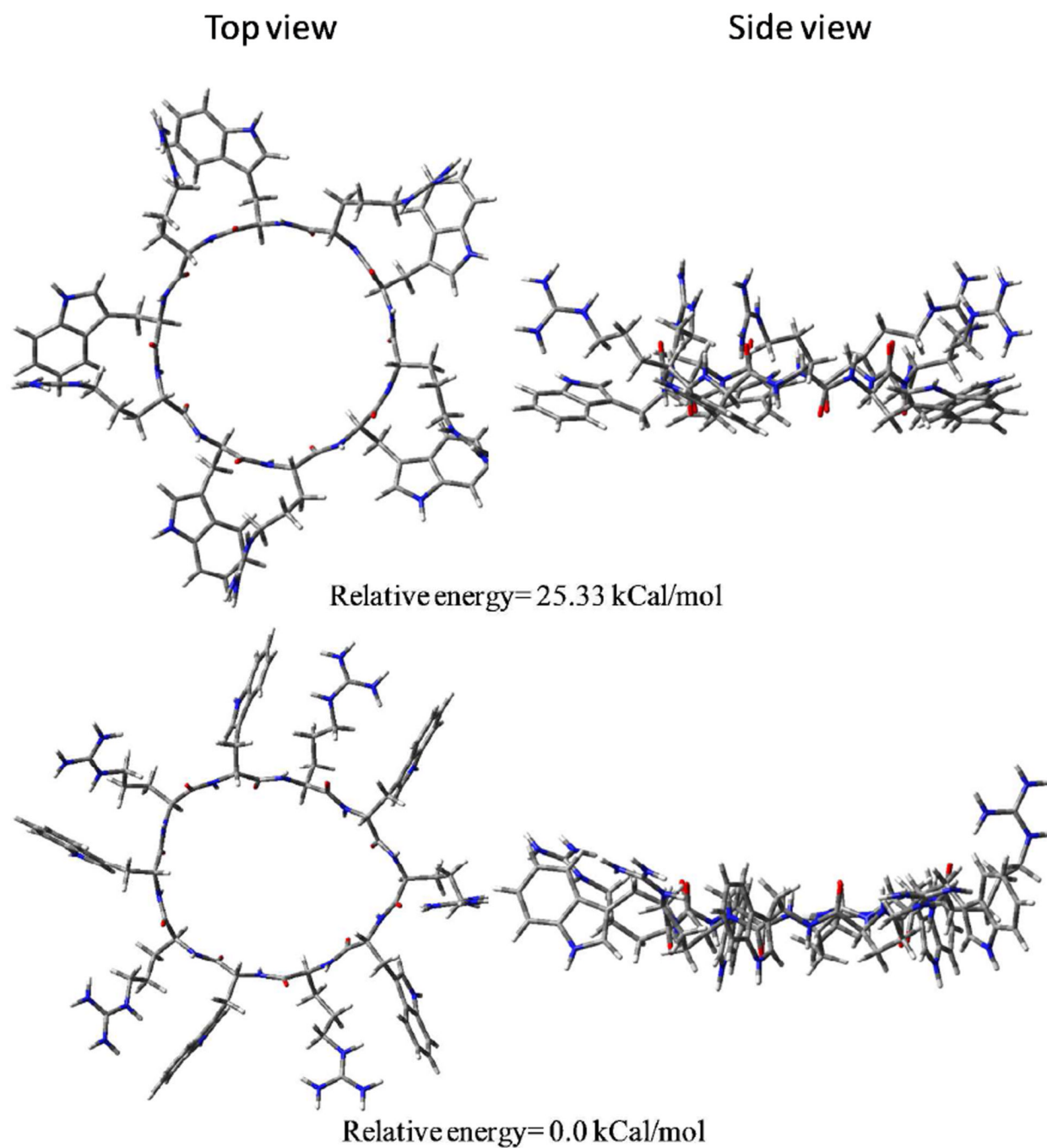


**Figure 8.**  
 (a) Negatively stained TEM images of  $[WR]_4$  (1 mM), PEpYLGLD (1 mM), and PEpYLGLD-loaded  $[WR]_4$  (1 mM) in water after one day; (b) Proposed mechanism of interactions between PEpYLGLD and  $[WR]_4$ .



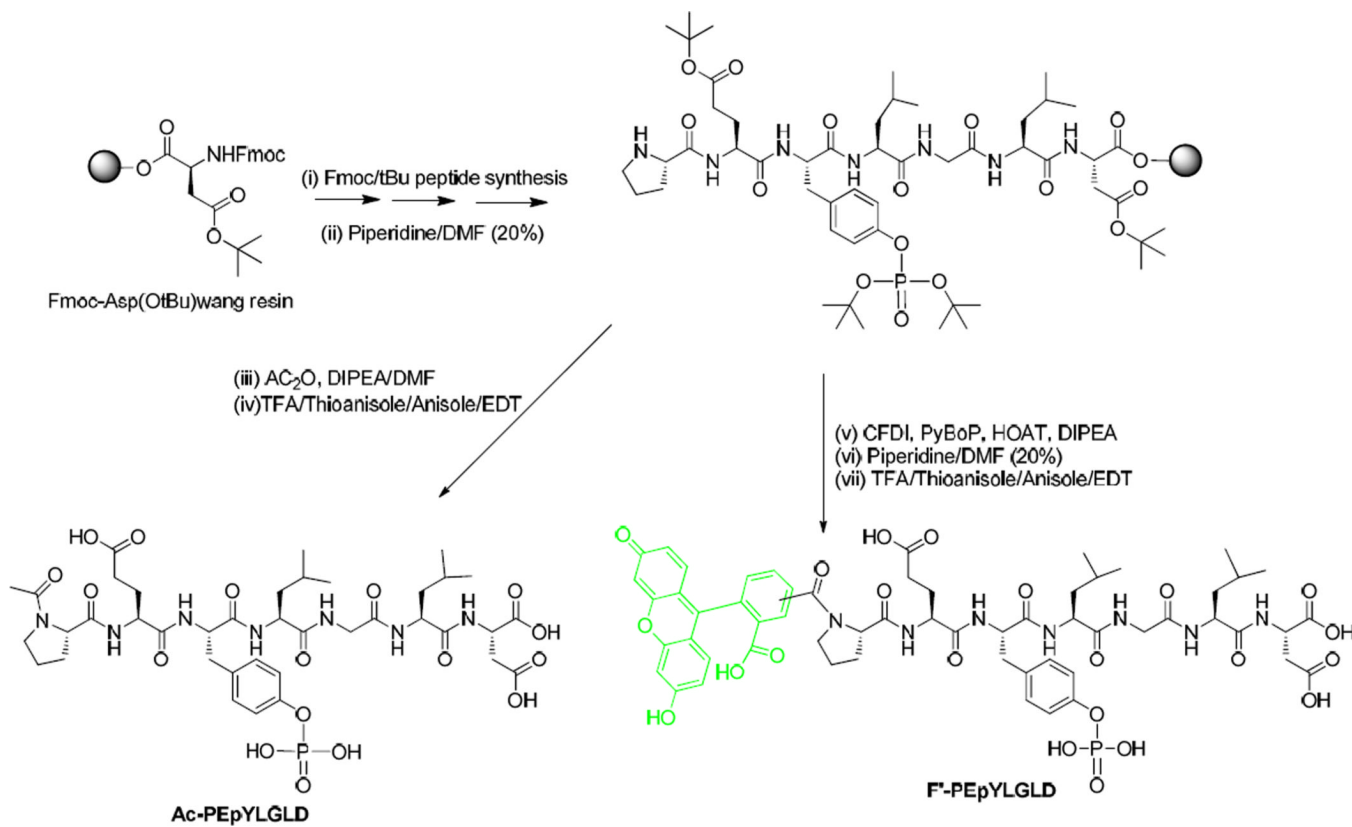
**Figure 9.**  
The binding isotherm obtained from titration of PEpYLGLD (6 mM) with [WR]<sub>4</sub> (500 μM) using a three sequential-binding sites model.





**Figure 10.**  
Two different conformers of [WR]<sub>5</sub>.





**Scheme 1.**  
Solid-phase synthesis of Ac-PE(pY)LGLD and F'-PE(pY)LGLD.